**Atmospheric
Chemistry
and Physics**

# Measurement and simulation of the 16/17 April 2010 Eyjafjallajökull volcanic ash layer dispersion in the northern Alpine region

**S. Emeis[1], R. Forkel[1], W. Junkermann[1], K. Schäfer[1], H. Flentje[2], S. Gilge[2], W. Fricke[2], M. Wiegner[3], V. Freudenthaler[3], S. Groß[3], L. Ries[4], F. Meinhardt[4], W. Birmili[5], C. Münkel[6], F. Obleitner[7], and P. Suppan[1]**

[1]Institute for Meteorology and Climate Research (IMK-IFU), Karlsruhe Institute of Technology,
Garmisch-Partenkirchen, Germany
[2]DWD German Meteorological Service, Offenbach and Hohenpeißenberg, Germany
[3]Meteorological Institute, Ludwig-Maximilians-Universität Munich (MIM), Germany
[4]UBA Federal Environmental Agency, Germany
[5] Leibniz Institut für Tropospheric Research, Leipzig, Germany
[6]Vaisala GmbH, Hamburg, Germany
[7]IMG-IBK Institute for Meteorology and Geophysics, University of Innsbruck, Austria

**Abstract.** The spatial structure and the progression speed of the first ash layer from the Icelandic Eyjafjallajökull volcano which reached Germany on 16/17 April is investigated from remote sensing data and numerical simulations. The ceilometer network of the German Meteorological Service was able to follow the progression of the ash layer over the whole of Germany. This first ash layer turned out to be a rather shallow layer of only several hundreds of metres thickness which was oriented slantwise in the middle troposphere and which was brought downward by large-scale sinking motion over Southern Germany and the Alps. Special Raman lidar measurements, trajectory analyses and in-situ observations from mountain observatories helped to confirm the volcanic origin of the detected aerosol layer. Ultralight aircraft measurements permitted the detection of the arrival of a second major flush of volcanic material in Southern Germany. Numerical simulations with the Eulerian meso-scale model MCCM were able to reproduce the temporal and spatial structure of the ash layer. Comparisons of the model results with the ceilometer network data on 17 April and with the ultralight aircraft data on 19 April were satisfying. This is the first example of a model validation study from this ceilometer network data.

## 1 Introduction

The emission of geogenic material and smoke and their dispersion in the atmosphere have always affected human societies. Except from the luckily rare occasions of meteorite impacts (see, e.g., Pollack et al., 1983), the most prominent types of these events are the advection of material from wind erosion such as desert dust (Shao, 2008), from large fires (Damoah et al., 2004), and from volcanic ash plumes (Woods et al., 1995) over populated areas. All these types of events can lead to reduced incoming shortwave radiation, reduced visibility, and even – in extreme cases – to adverse health impacts and degradation of specific instrumentation such as jet aircraft turbines.

In Europe, desert dust advection from the Sahara happens now and then on the front side of approaching troughs from the West (Ansmann et al., 2003). These events, which are sometimes visible to the human eye as colourless haze in higher atmospheric layers, rarely affect the normal life of biota. Aviation over Europe is usually not affected by Saharan dust, although Simpson et al. (2003) do not rule out impacts of Asian dust on aviation. The advection of volcanic ash clouds on the other hand has led several times to remarkable effects on air traffic due to the lower melting point of ejected material as compared to desert dust (Casadevall, 1992), and due to the sharp-edged nature of the emitted particles (see, e.g., Tupper et al., 2006 for a list

*Correspondence to:* S. Emeis
(stefan.emeis@kit.edu)

of some studies on past events). In order to avoid damage to and the failure of aircraft in operation, a global network of nine Volcanic Ash Advisory Centres (VAAC) was established in the 1990s (ICAO, 2000). The dispersion of volcanic ash clouds over Northern and Central Europe is currently computed by the Lagrangian model NAME (Numerical Atmospheric-dispersion Modelling Environment) and the simulation results are interpreted and issued by the London VAAC (Witham et al., 2007).

A prominent event of a tropospheric advection of volcanic ash over Europe was after the eruption of the Icelandic volcano Laki in Iceland which commenced on 8 June 1783 and lasted until 8 February 1784. This was the most violent, extensive and prolonged volcanic episode which has occurred in the Northern Hemisphere during the modern era (Grattan and Brayshay, 1995). The volcano generated $SO_2$ at a rate of 1.7 million tonnes per day during the first 6 weeks of the eruption. In addition, huge amounts of hydrofluoric and hydrochloric acid were emitted during this period. The resulting "dry fog" was present nearly constantly during late June, July, and August of 1783 in Britain, Scandinavia, France, Belgium, the Netherlands, Germany, and Italy, where it shrouded the sun and moon, reduced visibility, affected human health, and withered vegetation. Air-pollution concentrations during this 18th century event were at least as great as those recorded during modern urban air-pollution episodes, and these conditions probably persisted or recurred throughout Europe during the summer of 1783 (Durand and Grattan, 2001).

On 14 April 2010, the Icelandic volcano Eyjafjallajökull erupted fiercely and its ash cloud was advected by northwesterly winds towards Central Europe. The ash cloud was not observable by the naked eye, but nevertheless it had a massive impact on the European air traffic. Aircraft were grounded in most parts of Europe for more than five days between 15 April and 21 April 2010. The traffic bans for different parts of Europe were based mainly on the forecasted ash cloud dispersion from the London VAAC dispersion model. Thus, the assessment and forecasting of the spatial structure and the dispersion of such volcanic clouds has become a major public issue affecting the broader economy, in particular the aviation industry.

This paper will cover the detection and analysis of the spatial structure and dispersion of the volcanic ash cloud mainly by optical ground-based remote sensing, some insitu air quality measurements in Southern Germany close to the Alps, and a Eulerian dispersion model simulation with MCCM (Grell et al., 2000). The analysis will concentrate on the propagation of the first southward-moving ash cloud which arrived over Germany on 16 and 17 April 2010. It will report on its detection by a ground-based remote sensing network and address the identification of the volcanic origin of the detected aerosol cloud. The influence of the Alps at the southern frontier of Germany on the ash dispersion will be briefly investigated. Finally, the remote sensing network

**Table 1.** Eruption characteristics of Eyjafjallajökull from Petersen (2010) and http://www.earthice.hi.is/page/ies_Eyjafjallajokull_eruption.

| | |
|---|---|
| 14 April: | eruption plume rose to up to 9.5 km height deflected to the east by westerly winds |
| 16 April: | pulsating eruptive plume reaches above 8 km, with overall height of 5 km |
| 17 April: | eruption plume loaded with tephra (ash) rises to more than 8 km |
| 21 April: | plume height 3 km |
| 22 April: | the plume reached temporarily up to 6 km height |
| 23 April: | the plume was mostly at about 3 km level. |

data will be used to verify a dispersion simulation with the Eulerian model.

We will not discuss subsequent regional or global dimming effects or any other climate impact issue, because Eyjafjallajökull only ejected material into the troposphere. A related paper by Schäfer et al. (2011) will analyse the interaction between the ash cloud and the atmospheric boundary layer and focus on air quality and health issues.

## 2 Data, weather situation, and instruments

### 2.1 2010 Eyjafjallajökull activity

The Eyjafjallajökull is a 1666 m high ice-covered volcano near the southern tip of Iceland at 63°38′ N, 19°36′ W. A minor eruption had already occurred earlier in 2010 with the major outbreak occurring on 14 April 2010 and activity lasting until 22 May 2010. Since then, only water vapour has been emitted from the volcano. Some details of the first days of this eruption are listed in Table 1. This information serves to characterize the strength and height of the eruption since quantitative emission data is not available. The ejected material from the major eruption on 14 April 2010, which was also the fiercest, will be the focus of this paper.

### 2.2 Weather situation

The transport of volcanic ash clouds from volcanoes in Iceland towards Central Europe depends on the height of the eruption cloud and the prevailing wind patterns over Western, Northern, and Central Europe. The eruption height of Eyjafjallajökull was between 3 km minimum and 9.5 km maximum (Petersen, 2010, see also Table 1). This led to an injection of material into the middle and partly also upper troposphere but not into the stratosphere. The mean emission

height roughly coincided with the height of the 500 hPa layer of the troposphere.

Therefore, Fig. 1 (left) shows the flow patterns in this 500 hPa layer at 48 h intervals from the period with air traffic bans. It shows a rather stationary weather situation with high pressure over the Atlantic and the British Isles, a weak and decaying trough over Central and Southwestern Europe and anticyclonic activity to the North. From 19 April onwards, a trough over Scandinavia was forming. Remarkable is the persisting low wind speed situation over Central Europe. This led to the phenomenon that the ash cloud, which had been advected towards Central Europe between 14 April and 17 April, remained and decayed there for several days before it was finally completely removed by westerly winds from 21 April onwards.

The right-hand column in Fig. 1 shows the predictions of the London VAAC based on simulations with the Lagrangian dispersion model NAME. It simulated a transport of volcanic ash towards Scandinavia on the first day after the eruption. Two days later, the core of the ash cloud was simulated to have moved southward, consequently covering the whole of Central Europe. A partial transport of ash back towards the Atlantic due to the anticyclonic (clockwise) circulation over the British Isles is visible as well. In the following days, the cloud was more or less stagnant over Central Europe, but started to disappear on 21 April so that the flight ban could be lifted on this day.

## 2.3 Measurement instruments

Instrumentation, which delivered the data for the present assessment includes optical surface-based remote sensing devices over Germany and Tyrol (Austria) and a few ground-based in-situ instruments in Southern Germany and onboard an ultralight aircraft. Measurement sites are shown in Fig. 2.

### 2.3.1 Optical remote sensing

The ceilometer network of the German Meteorological Service (DWD), which now consists of 36 Jenoptik CHM15K instruments operating at 1064 nm allows for an areal observation of aerosol backscatter over Germany (Flentje et al., 2010a, b). Here, data from Augsburg, Weihenstephan and Hohenpeißenberg are used. These biaxial ceilometers provide vertical profiles of particle and molecular backscattering in an atmospheric column from about 600 m above ground level up to 15 km with a vertical resolution of 15 m at a 5–7 kHz repetition rate. The wavelength of 1064 nm provides relatively large contrast to molecular scattering, thus highlighting aerosol structures. However, the scattering efficiency drops sharply for particles with radii well below 1 μm, which limits the accuracy of a single profile. See Flentje et al. (2010b) for additional data from a VAISALA LD-40 ceilometer, operated at the Schneefernerhaus on the Zugspitze, and further references.
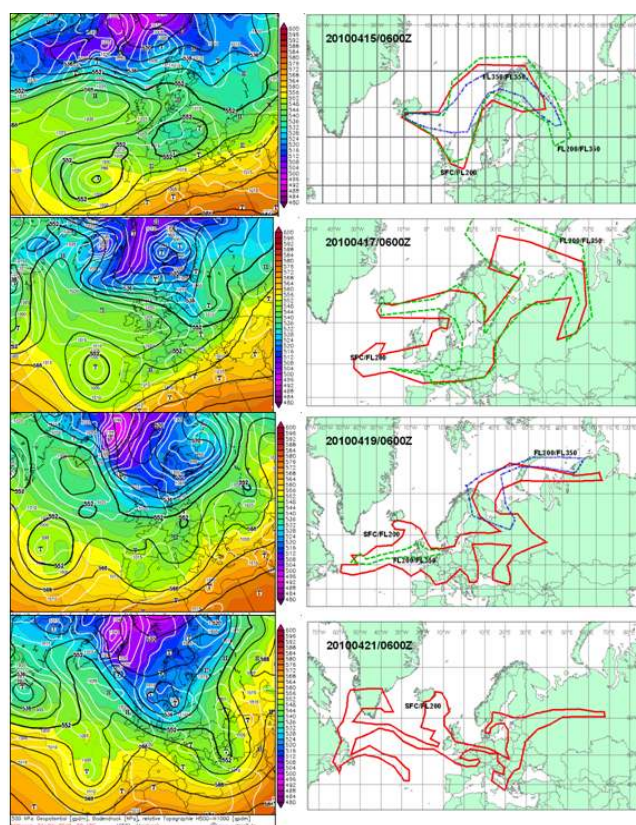


**Fig. 1.** Left: 500 hPa maps of Europe for 15, 17, 19, and 21 April 2010, 00:00 UTC (Source: http://wetter3.de). Black lines: 500 hPa isolines in gpdm, colours: temperature in °C. Right: Six-hour forecast of the extent of the ash cloud for 15, 17, 19, and 21 April 2010, 06:00 UTC from the internet presentation of the London VAAC (VAAC use a dynamic map as background changing from day to day).
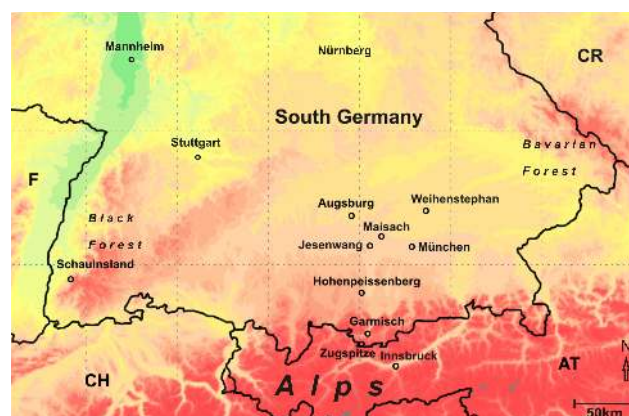


**Fig. 2.** Map showing the measurement locations in the northern Alpine region. Shading represents orography.

The quantitative assessment of optical properties of the volcanic ash layer is derived from lidar measurements (MIM) performed in the framework of EARLINET (see, e.g., Bösenberg et al., 2003). In the present paper, data from the multi-wavelength lidar system MULIS (e.g., Freudenthaler et al., 2009) in Maisach is considered. MULIS is a Raman-depolarization lidar including channels for elastic backscattering at 355 nm, 532 nm, and 1064 nm, and the corresponding Raman channels at 387 nm and 607 nm. The linear depolarization ratio of particles, $\delta_p$, is derived at 532 nm. The optical design of the lidars is optimized for measurements in the troposphere, i.e., MULIS provides data from 200 m up to 4000 m above ground level depending on field stop adjustments. The range resolution of the raw data is 7.5 m and the temporal resolution is typically 10 s. Observations were made at Maisach, a rural site 25 km north-west of Munich.

In addition, a biaxial JenOptik CHM15kx ceilometer was continuously monitoring the aerosol stratification over downtown Munich at the site of the MIM. The emitted wavelength is 1064 nm, the range resolution is 15 m, and the temporal resolution is 30 s. In contrast to the ceilometers of the DWD network described above (CHM15k instruments), this ceilometer provides aerosol data from above approximately 200 m above ground. As a consequence, it is better suited for sounding the lower part of the atmosphere than the CHM15k ceilometer and thus giving information about the convective evolution of the boundary layer.

The Garmisch-Partenkirchen branch of the Institute of Meteorology and Climate Research of Karlsruhe Institute of Technology (IMK-IFU) has been operating a mono-axial Vaisala CL31 at Augsburg city centre since 2008. The Austrian flight controlling authority (Austro Control GmbH) operates several Vaisala CL31 ceilometers in the Inn Valley near Innsbruck (and at the airport Vienna Schwechat), the data from which have been analysed by the Institute of Meteorology and Geophysics of the University of Innsbruck, Austria (IMG-IBK). This ceilometer is a one-lens ceilometer using infrared light of 910 nm. It offers a height resolution of 10 m from about 30 m above ground to a maximum range of 7500 m. A comparison of the optical configuration of mono-axial and biaxial ceilometers can be found in Emeis (2010).

### 2.3.2 In-situ instruments

The ultralight aircraft of IMK-IFU flew in the area of Augsburg in the late afternoon of 19 April 2010. This research aircraft is based on a weight shift ultralight (Junkermann, 2001) and is equipped with a suite of instruments for the measurement of aerosol and radiation properties, ozone and meteorological parameters. Instrumentation relevant for the detection of the volcanic ash cloud consists of an optical particle counter GRIMM 1.108 with 15 size bins between 300 nm and 20 µm, an open path nephelometer for the measurement of the extinction, and a seven- wavelength aethalometer, MAGEE AE42, for the spectral characterisation of the

aerosol. The flight was performed about 10 km northwest of the airport of Jesenwang (48°10.46′ N, 11°10.50′ E, between Munich and Augsburg) with the intention to be comparable to the ceilometer and LIDAR measurements in the vicinity.

Surface-based ancillary measurements of gases and aerosol properties were taken from routine observations performed at Schauinsland station at 1200 m a.s.l. by the German Environmental Agency (UBA). Schauinsland is a summit site in the southern Black Forest in the southwestern corner of Germany. $SO_2$ is measured with a TE43CTL Thermo Scientific, $PM_{10}$ with a Thermo Fisher FH62IR. The particle size spectrum is obtained from a scanning mobility particle sizer (SMPS) with a range from 10–800 nm (differential mobility analyser from IFT, Leipzig, with condensation particle counter CPC 3772). The size spectrum sample has been differentiated by an alternating treatment with and without a thermo-denuder at 300 °C. The black carbon content of aerosol was measured with a MAAP (Multi Angle Absorption Spectrometer MLU 5012).

Aerosol measurements at the UBA station at Schneefernerhaus close to the Zugspitze at an altitude of 2650 m a.s.l. are carried out with a SMPS (model TSI 3080 with condensation particle counter 3010 CPC) for number concentrations of particle size distribution from 10–800 nm. The continuous quality assurance of measured number concentrations for the size distributions has been done with parallel measurements of TSI 3772 butanol and TSI 3785 water CPC. A chemical analysis is made for $SO_2$ with a Thermo Scientific TE43i TLE (operated by DWD) and for black carbon with a MAAP (MLU Carusso, Model 5012). Forward and backward scattering coefficients are obtained with a three-wavelength integrating nephelometer TSI 3563.

Additionally, at both stations, $PM_{10}$ daily samples with a Digitel HiVol sampler have been collected. For mass determination, 22 cm filters were equilibrated, premeasured, transferred to the measuring site, and after sampling brought back to the central lab. After a renewed equilibration, the second measurement for the determination of mass difference was performed.

For Innsbruck, half hourly data of the concentration of $SO_2$ und $PM_{10}$ were provided by the Umweltbundesamt GmbH, Austria.

### 3 Dispersion model MCCM

The online coupled meteorology atmospheric chemistry model MCCM (Grell et al., 2000) is a meso-scale flow simulation and weather forecast model based on the 5th-generation Penn State/NCAR Mesoscale Model (MM5, Grell et al., 1994) frequently used for investigations of air quality during episodes, real time weather and air quality forecasts, as well as for the investigation of climate impact on regional air quality. It includes a choice of three gas phase chemistry modules (Haas et al., 2010). MCCM has been operated here

with the RADM gas phase chemistry (Stockwell et al., 1990). Aerosol processes are described with the modal aerosol module MADE/SORGAM (Schell et al., 2001) which distinguishes three modal size distributions. The description of the Aitken mode and the accumulation mode processes includes the inorganic as well as organic compounds and considers interactions with the gas phase. For the coarse mode, sedimentation is taken into account but no interaction with the gas phase is considered. For the simulations of the volcanic ash dispersion, the ash was attributed entirely to the coarse mode and handled as mineral dust in MADE/SORGAM.

The simulations starting on 14 April 00:00 UTC were set up for the whole of Europe with a horizontal resolution of 25 km ($199 \times 169$ grid points). The atmosphere between the surface and the 50 hPa level is resolved in 33 layers, with a vertical resolution that decreases with height. The thickness of the lowest layer is 30 m near the ground and in the free troposphere the layers are between 450 m and 700 m thick.

The emission of ash from the volcano is considered in the model to occur within a vertical column of variable height. The top of the emission plume is modulated according to the published plume height measured by the weather radar operated by the Icelandic Met Office (Petersen, 2010, see also Table 1). The emission source strength of airborne material during the first 3 days of the eruption was assumed to be 5% of the published amount of tephra ($140 \times 10^6 \, m^3$). Depending on the observed plume height, this corresponds to a mineral aerosol emission from $100\,000\,t\,h^{-1}$ to $500\,000\,t\,h^{-1}$. Furthermore, a $SO_2$ source of $1000\,t\,h^{-1}$ to $5000\,t\,h^{-1}$ was arbitrarily assumed.

# 4 Proof of the volcanic origin of the cloud

Before we present the results from the remote sensing network and the numerical simulations, we have to verify the volcanic origin of the observed aerosol cloud. This is necessary, since ceilometer observations measure a pure backscatter intensity that does not allow for a distinction between nearly spherical particles such as small boundary-layer aerosol particles and non-spherical sharp-edged particles such as volcanic ash particles. Three different approaches to validate the volcanic origin of the aerosols detected by the ceilometers are pursued here: (1) from the depolarisation ratio obtained with advanced lidars (Wiegner et al., 2011), (2) from back trajectories from GME analyses of DWD, (3) from the simultaneous increase of $SO_2$ and particle concentrations at mountain observatories upon arrival of the cloud.

## 4.1 Investigation with depolarisation lidars

Profiles of the particle linear depolarisation ratio, the backscatter coefficient and the extinction coefficient can be derived from data of the Raman-depolarization li-
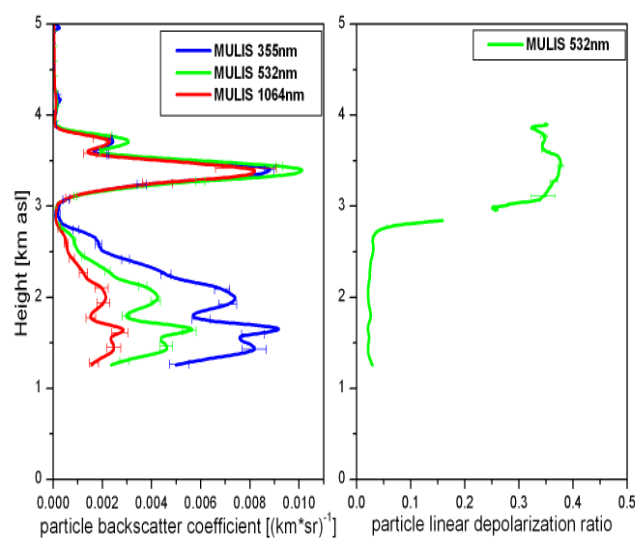


**Fig. 3.** One-our average of particle backscatter coefficient (left, in $(km\,sr)^{-1}$) and linear depolarisation ratio (right) from MULIS measurements at Maisach on 17 April 2010, 02:00 UTC.

dar MULIS. Figure 3 shows – as an example – optical properties from measurements on the early morning of 17 April 2010 (02:00 UTC). The left frame, displaying the particle backscatter coefficients at three wavelengths, indicates the existence of two layers with increased aerosol content. The lower layer below about 2 km a.s.l. is characterized by a strong wavelength dependence of the backscatter coefficient, typical for particles of the residual layer from the boundary layer evolution of the preceding day. In contrast, the backscatter coefficient of the elevated layer around 3.5 km a.s.l. shows no wavelength dependence, indicating large particles. Similar conclusions are derived from extinction coefficient profiles (not shown here). The right-hand frame, displaying the particle linear depolarisation ratio, reveals a remarkable difference between these two layers. Whereas the backscatter from the lower layer exhibits nearly no depolarisation, the upper layer signal is considerably depolarised. This very high depolarisation ratio of almost 0.4 is a strong evidence for the presence of non-spherical particles such as that expected from a volcanic eruption.

## 4.2 Back trajectories

The origin of an air mass may be analysed from the measured wind field and from back trajectories. Analyses of vertical wind from ECMWF (European Centre for Medium-Range Weather Forecasts, Reading, UK, Fig. 4) and DWD global model back trajectories (Fig. 5) indicate that the aerosol cloud which arrived at Hohenpeißenberg observatory of the German Meteorological Service southwest of Munich was advected as an initially higher elevated tilted layer and simultaneously subsided by about 1–2 km per day while crossing Germany on 17 April 2010. The meteorological analysis
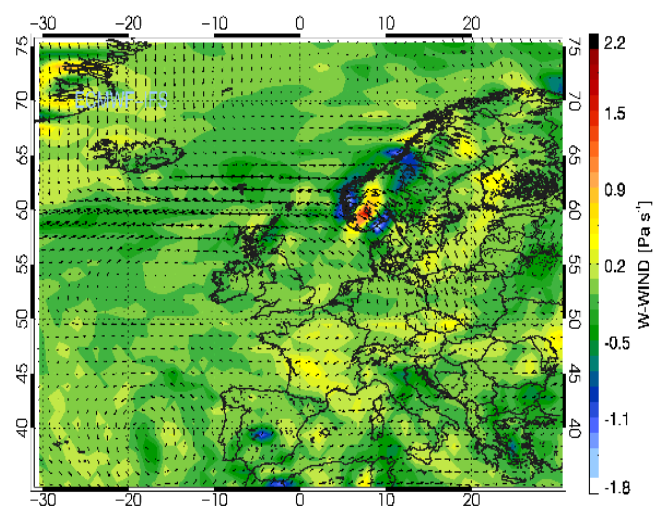
**Fig. 4.** Horizontal winds (arrows) and vertical winds (colours, in Pa s$^{-1}$, positive is downward) at 500 hPa on 17 April 2010, 12:00 UTC (ECMWF analysis).
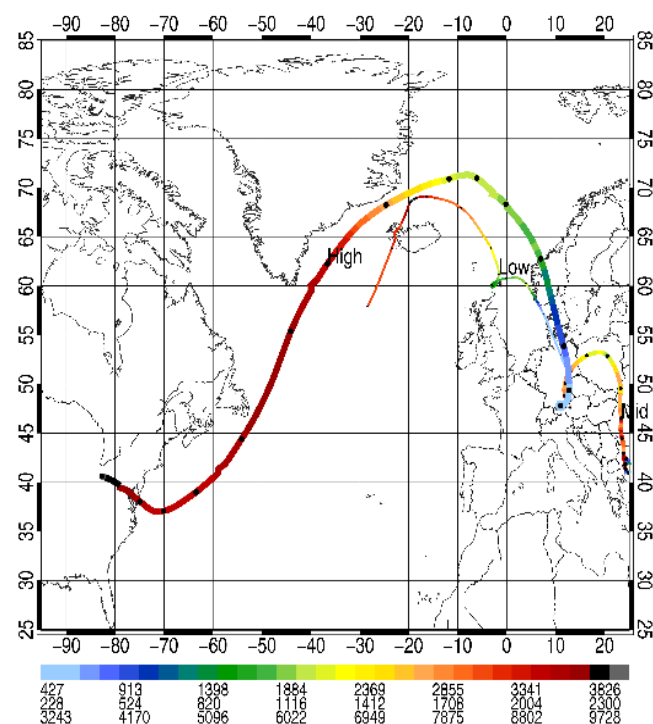


**Fig. 5.** Back trajectories arriving at Hohenpeißenberg (HPB) observatory at low (thin, arriving at HPB about 800 m a.s.l., upper row of colour bar annotation), medium (arriving at about 1500 m a.s.l., middle row of colour bar annotation), and high level (thick, arriving at HPB about 3000 m a.s.l., lower row of colour bar annotation) on 17 April 2010, 18:00 UTC. Black dots on the trajectories mark 12 h intervals. The trajectories have been computed with the GME model of the German Meteorological Service.

(Fig. 4) shows a vertical velocity of 0.3 Pa s$^{-1}$ (0.1 Pa s$^{-1}$) corresponding to a subsidence rate of about 2000 m (700 m) per day at 500 hPa (700 hPa). The DWD GME trajectory (Fig. 5) indicates a similar descent rate from about 4000 m to 3200 m (each a.s.l) during the 24 h before arrival at Hohenpeißenberg. Also the back trajectories indicate that this was about 1000 m per day (roughly 0.01 m s$^{-1}$). Simultaneously, Fig. 5 shows that the ash travelled about 1000 km in 24 h horizontally before arriving at Hohenpeißenberg. The thick curve in Fig. 5 (labelled "High", arriving at about 3000 m a.s.l. at Hohenpeißenberg) indicates that the air mass at about 2.5 km height carrying the ash over the Hohenpeißenberg on 17 April 18:00 UTC very probably had passed Iceland three days ago. Thus a volcanic origin of the ash load in this air mass is very likely.

### 4.3 Comparison to surface measurements

Apart from aircraft measurements with the Dimona of Metair in Switzerland on 17 April (see www.metair.ch), observations at mountain tops were the only means that permitted an in-situ proof of the volcanic nature of the first advected dust particles detected by the ceilometers, before the ash material was included into the atmospheric boundary layer (see Schäfer et al., 2011). The flights of the Falcon of DLR, Germany (Schumann et al., 2010), and the ultralight aircraft data addressed in Sect. 5.2 did not take place before 19 April.

Figure 6 reports in-situ aerosol parameters that were recorded on 17 and 18 April 2010 at Zugspitze and Schauinsland. The two upper graphs show particle number size distributions recorded with Scanning Mobility Particle Sizers (SMPS) within the German Ultrafine Aerosol Network (Birmili et al., 2009). Zugspitze features a significant increase in ultrafine (mobility diameter $Dp > 60$ nm) particle concentration at 09:30 UTC on 17 April. Meanwhile there is a modest increase in accumulation mode concentration (100 nm $< Dp < 600$ nm). Schauinsland shows a very similar increase in ultrafine particle concentration about two hours later. The delay at Schauinsland is probably due to the much lower height (1200 m compared to the 2670 m of the Global Atmospheric Watch (GAW) station close to the peak of the Zugspitze). At both sites, the ultrafine particle bursts were associated with a significant entrainment of sulphur dioxide (for Schauinsland, see bottom graph of Fig. 6). It is very likely that the ultrafine particles were generated in the volcanic plume by gas-to-particle formation, i.e., more specifically, by the photochemical formation of sulphuric acid from sulphur dioxide and subsequent particle nucleation.

Apart from the ultrafine particle burst, there were only modest indications of the entrainment of fine ($Dp < 1$ μm) particles. In the afternoon of 17 April, the PM$_1$ mass concentration calculated from the SMPS data, assuming a particle density of 1.6 g cm$^{-3}$, reached 25 μg m$^{-3}$. Similar PM$_1$ values prevailed at Schauinsland (bottom graph of Fig. 6).
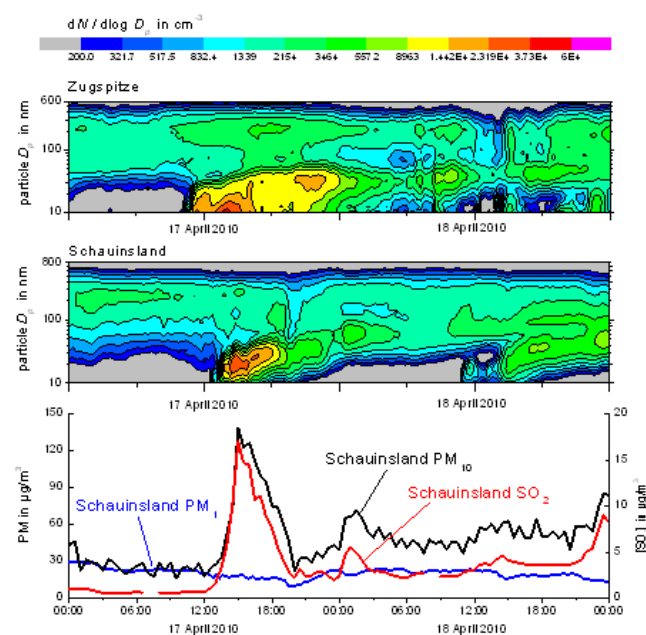
**Fig. 6.** Particle number size distributions at Zugspitze (top) and Schauinsland (center) on 17 and 18 April 2010, and time series of PM$_{10}$ and PM$_1$ mass concentration, and sulphur dioxide at Schauinsland (below). The number size distribution plots combine time (x-axis), particle diameter (y-axis) and particle number concentration in dN/dlogDp (colour coding).

These values are, in fact, rather typical for the lower troposphere and do not indicate the exclusive presence of a volcanic aerosol. Striking evidence for the entrainment of volcanic ash was, however, indicated by the time series of PM$_{10}$ mass concentrations. The gravimetrically determined PM$_{10}$ concentration reached 140 μg m$^{-3}$ at Schauinsland in the afternoon of 17 April (Fig. 6) and around 35 μg m$^{-3}$ at Zugspitze. At Schauinsland, PM$_{10}$ exceeded PM$_1$ by a factor of around 6. A PM$_{10}$/PM$_1$ ratio of 6:1 strongly indicates the presence of coarse particles ($Dp > 1$ μm). Such a ratio is unusually high for the troposphere, and therefore suggests the entrainment of volcanic ash particles. Evidence for these particles originating from the volcanic plume is given by the extremely high correlation between PM$_{10}$ and sulphur dioxide concentration (Fig. 6). When comparing the PM$_{10}$ levels, it appears that more volcanic ash was entrained at Schauinsland compared to Zugspitze. This might be indicative of spatial heterogeneities in the volcanic plume. This effect as well as further details of the interaction of the ash cloud with surface air quality are explored in a forthcoming paper by Schäfer et al. (2011).
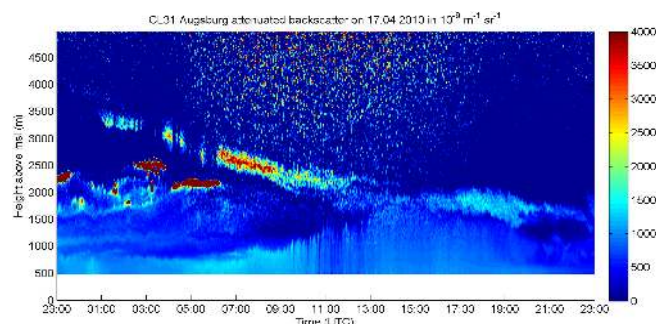


**Fig. 7.** Attenuated backscatter at 910 nm measured with a CL31-Ceilometer of IMK-IFU at Augsburg city centre on 17 April. Heights are given in m above sea level. Dark blue: very low backscatter, red: higher backscatter, brown: very high backscatter (water clouds). The ash cloud provoked the slanted echoes from upper left to lower right.

# 5 Analysis of the temporal and spatial structure of the cloud

## 5.1 Remote sensing observations

Remote sensing with ceilometers gives time-height cross-sections of the optical backscatter intensity. A typical result from such an instrument is shown in Fig. 7 which is explained in a bit more detail here. It shows one day of range-corrected but otherwise uncalibrated optical backscatter intensity observed at Augsburg, Southern Germany on 17 April 2010. The most striking feature is the slanted filament-like structure of a shallow ash layer of several hundreds of metres thickness visible during the first half of the day descending from about 3500 m a.s.l. to about 2000 m a.s.l. at noon. This seems to show an apparent sinking of the ash layer of about 3000 m per day. But referring to Sect. 4.2 the sinking motion is only of the order of 1000 m per day. Therefore, the rest (2000 m per day) of the apparent sinking must be attributed to a slanted orientation of this ash layer that is advected over the ceilometer site. This means that the leading edge of the ash layer over Augsburg was at about 3500 a.s.l. while that part of the ash layer 500 km upstream, which was to arrive at Augsburg about 12 h later, was at 2500 m a.s.l. This gives an inclination of the shallow ash layer in the lower troposphere over Germany of about 1:500.

The brownish-red structures at 2000 to 2500 m a.s.l. in the very left of Fig. 7 are normal water clouds. Also, the structures underneath these clouds are not related to the volcanic ash. Those clouds obstruct the view of the instrument of the layers above the clouds. Therefore, the detection of the shallow ash layer above is interrupted for the periods in which lower-level clouds appeared.

The development of the boundary layer is also visible from CL31 soundings as the one displayed in Fig. 7. The increasing depth of this layer can be followed from the lighter

blue area adjacent to the surface which reaches its maximum depth in the later afternoon at more than 1000 m. The detection of the boundary layer is due to the enhanced aerosol content in this layer originating from surface sources. Figure 3 has demonstrated that the near-surface aerosol in this lower layer does not show any depolarisation. Therefore, this near-surface aerosol is definitely not of a volcanic origin. Figure 7 also shows that the ash cloud was not mixed into the boundary layer at Augsburg that afternoon, because a very narrow dark line remains faintly visible between the backscatter due to the ash aloft and the backscatter due to the boundary-layer aerosol.

The arrival of the volcanic ash layer over Germany on 15/16 April was documented by all ceilometers of the DWD ceilonet (Flentje et al., 2010b) and the other ceilometers and lidars used in this study. Figure 8 shows measurements in Southern Germany at Augsburg, Weihenstephan, Hohenpeißenberg (DWD-Ceilonet, CHM15k), at Munich (MIM, CHM15kx), and the MIM-lidar at Maisach with a slightly different colour code. Shown are the range corrected signals (1064 nm) as time-height cross-sections from 15:00 UTC (16 April) till 24:00 UTC (17 April). The vertical axis is height above sea level from 0 to 8 km.

The fourth frame in Fig. 8 shows time-height cross-sections as derived from MULIS at Maisach. The layer could be clearly observed from 17:00 UTC at an altitude of more than 7 km. The measurements were subsequently interrupted for two hours and partly influenced by low clouds. Nevertheless, the temporal evolution of the ash layer could clearly be demonstrated. At midnight, the layer was detected at 4 km height; at 12:00 UTC on 17 April it was between 2 and 2.5 km and still clearly separated from the planetary boundary layer. The maximum signal over Maisach was observed between 05:00 and 09:00 UTC. Note that volcanic ash was present throughout the day at heights up to 7 km. As MULIS is a sophisticated aerosol lidar with, e.g., pulse energies of roughly four orders of magnitude larger compared to the ceilometers, these data can serve as reference.

The arrival of the ash layer at about 17:00 UTC in Augsburg at an altitude of 6–7 km is hardly visible due to obscuration of low level clouds, however, after 20:30 UTC, the layer is clearly visible. The height gradually decreases from 5 km to 2.2 km within 15 h. This observation is supported by the observations from the nearby CL31 ceilometer of IMK-IFU (Fig. 7, see also there for a distinction between sinking motion and the advection of a slanted layer explaining the observed decrease in height of the ash layer). The comparison of the upper frame of Figs. 7 and 8 gives an impression of the different information from these two different types of ceilometer. While the CHM15k give a somewhat clearer image for the free troposphere, the mono-axial CL31 also covers the development of the boundary layer during this day. This boundary-layer development is not discernable from the CHM15k data from Augsburg.
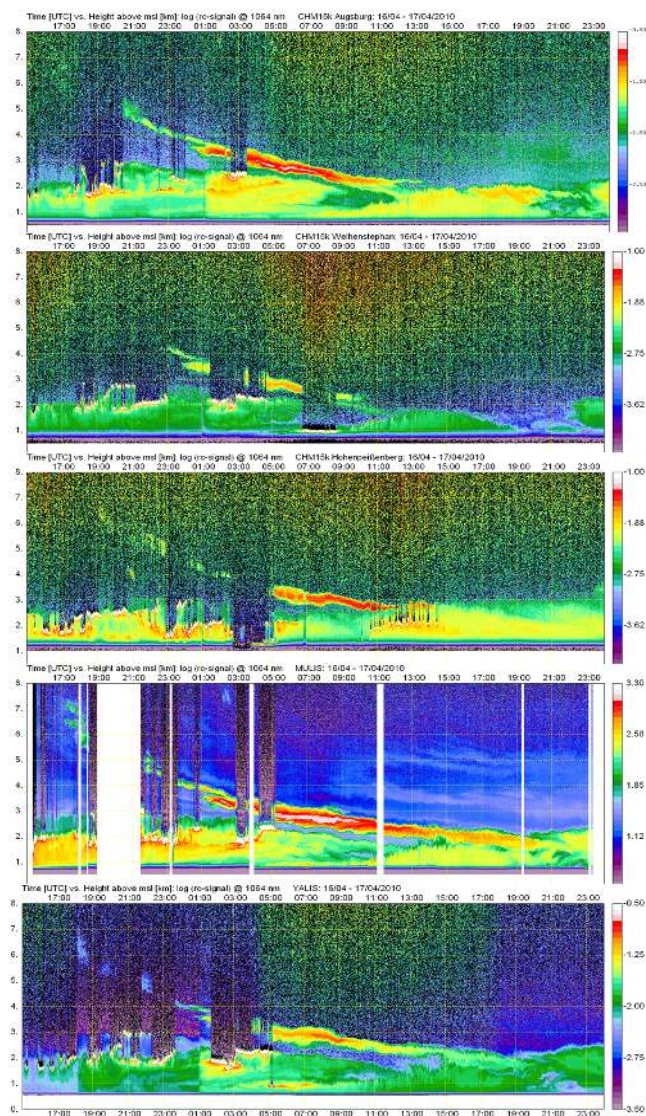


**Fig. 8.** Attenuated backscatter at 1064 nm at Augsburg (DWD, CHM15k), Weihenstephan (DWD, CHM15k), Hohenpeißenberg (DWD, CHM15k), Maisach (MIM, MULIS), and Munich (MIM,CHM15kx) (from top to bottom) from 16 April 2010, 15:00 UTC to 17 April, 24:00 UTC.

In Weihenstephan, the visibility of the ash layer was reduced due to a higher amount of low level clouds. The first observations were around 23:00 UTC on 16 April, from then the layer was visible with interruptions until 10:30 UTC, when it became indistinguishable from the boundary layer. In Munich, the volcanic ash could be observed since 18:00 UTC of 16 April with only short interruptions due to low level clouds. At 18:00 UTC, the ash layer was visible between 6 and 7 km. At 15:00 UTC (17 April), the layer got mixed with the planetary boundary layer in a height of 2.2 km. After 17:00 UTC, the aerosol of the volcanic eruption and the boundary layer could not be distinguished from
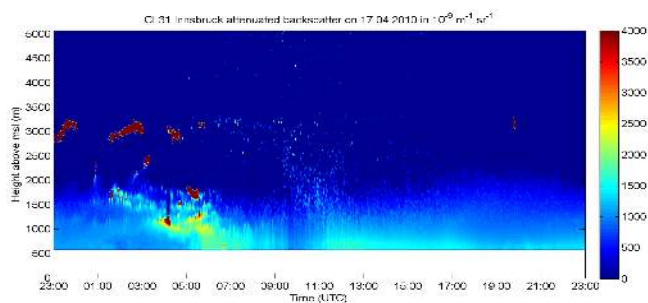
**Fig. 9.** As Fig. 7, but for Innsbruck.



**Fig. 10.** Vertical profiles of temperature, dew point, ozone and in-situ extinction coefficient (EXCO) on 19 April 2010 between 13:40 and 15:30 UTC. The red curve is from the ascent, the green curve from the descent of the aircraft. The aircraft position is about 10 km northwest of Jesenwang. The black line indicates the altitude of Jesenwang airfield.

the ceilometer data. The corresponding ceilometer data from Hohenpeißenberg are shown in the third frame of Fig. 8. The general trend of the development of the ash layer is similar to the one at Augsburg and Weihenstephan, however, the layer was visible from 19:00 UTC at about 6.5 km, i.e. somewhat later than at the other stations, due to the more southern position of this site. The faint ash layers above the main layer, which were seen by aerosol lidar MULIS, could not be observed by any of the ceilometers.

The ash cloud rapidly lost its identity when entering into the mountainous region of the Alps. Figure 9, taken at Innsbruck behind the first mountain chain of the Alps, only shows a weak signal which may be interpreted as optical backscatter from the ash cloud at about 3200 m a.s.l. between 06:00 and 10:00 UTC (see also Schreiter, 2010). It can be speculated that the strongly increased vertical exchange over the Alps (see, e.g., Furger et al., 2000 or Grell et al., 2000) leads to a rapid dilution of the ash cloud so that the ash concentration decreases and the sharp contours of the cloud decay. Synoptic weather analysis reveals that this development is also associated to a meso-scale low pressure system to the south of the Alps inducing a change from northeasterly to southerly wind directions and associated topographic subsidence at the northern fringes of the Alps. This interpretation is supported by consideration of regional radiosoundings (Innsbruck and Munich) which are characterized by a large spread and near adiabatic temperature gradients during the latter period. Moreover, enhanced $SO_2$ and $PM_{10}$ concentrations occurred at several locations in the area of Innsbruck during 17 April which was particularly pronounced in the early afternoon (Amt der Tiroler Landesregierung, 2010). Such surface concentration increases were not yet present in the foreland of the Alps on this day. These findings indicate topographically forced vertical mixing within the Alpine region in contrast to the situation in the Alpine foreland.

## 5.2 Probing the boundary layer with an ultralight aircraft

The ultralight aircraft took off at the airport of Jesenwang, 48°10,46′ N, 11°07,50′ E at 13:40 UTC for a vertical profile up to 4000 m a.s.l. and returned to the ground at 15:30 UTC

on 19 April 2010. The flight was performed about 10 km northwest of this airport with the intention of making comparable measurements with the ceilometer and lidar measurements in the vicinity. Unfortunately for logistical reasons, it was not possible to fly two days earlier. Luckily, the flight documented the front of another flush of volcanic material over Southern Germany with which it is worth comparing with numerical simulations of this event (see below). Therefore, a short analysis of this aircraft data is included here.

Due to the slow true airspeed of about 25 m s$^{-1}$, the flight pattern allows for focussing on the vertical distribution of the aerosols. The flight enabled a comparison between pre-volcanic aerosol and the volcanic ash plume, as it took place during the arrival of a new flush of volcanic ash. At an altitude of 3200 m a.s.l., a layer of 2/8 stratocumulus clouds and a temperature inversion was detected. Above this level clear skies prevailed. The aircraft maintained its maximum altitude of 3650 m a.s.l. for several minutes, followed by a slow descent back to ground. Between the ascent and descent, a clear exchange of the air masses was observed as shown in Fig. 10.

Most of the measured parameters changed significantly between the ascent and descent. The profiles of the dew point and extinction coefficient (Fig. 10b, c) indicate the arrival of a new air mass which was first seen in the ascending profile shortly before reaching the free troposphere, and later in the descending profile down to an elevation of about 500 m above ground. Data on particle size distributions are available only up to 2000 m a.s.l. in the ascent and below 1800 m a.s.l. in the descent. The number of large particles and the total suspended particle mass derived from the size distribution did not change significantly as it would have been expected from the change in the extinction coefficient (Fig. 11). This is an indication that the optical properties of the two air masses are different. Figure 11a–c shows the related optical absorption measured with the 7 wavelength aethalometer.
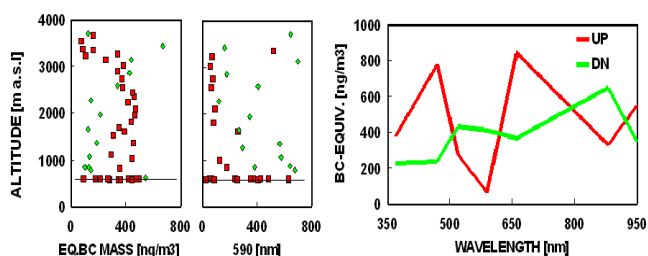
**Fig. 11.** Left: Vertical profiles of the individual values of spectral aerosol absorption at 370 nm and at 590 nm in black carbon equivalent mass. Right: Average spectral absorption (given in black carbon equivalent mass) for both profiles between 1000 and 3000 m a.s.l. Dates and site as in Fig. 10.

In Fig. 11 again, the red trace indicates the ascent, the green one the descent. Most striking within this data is the behaviour of the absorption at 370 to 420 nm and in the visible range at 590 nm. While in the ultraviolet the absorption decreased remarkably, the absorption in the visible increased. No significant difference was observed at the 880 nm wavelength, typically used for the detection of black carbon. Figure 11c gives the average absorption equivalent to black carbon mass in the seven channels. The aged air mass measured before arrival of the volcanic plume shows a bimodal structure with absorption in the UV and the near infrared with a minimum in the visible. This is typical for an aged air mass with some contribution of organic matter. The replacing air mass, expected to be of volcanic origin had a quite different spectral fingerprint. The smooth spectra with a slight increase in the absorption from the UV to the infrared is typical for a more homogeneous aerosol mixture like it is observed in layers of Saharan dust. It has also been seen previously during research flights in Mexico during the MI-LAGRO campaign (Grutter et al., 2008) during a passage a few hundred m below the sulphur dioxide plume of the volcano Popocatepetl. Summarizing these results indicates that from a particle-size point of view a volcanic ash plume would be difficult to identify. Therefore, the combined in-situ measurement of particle sizes, optical properties, and selected trace gases is a more promising approach. However, without aerosol chemistry measurements, a more robust identification of a volcanic plume would require at least the additional measurement of sulphur dioxide.

# 6   MCCM model results

The main focus of the MCCM simulation presented below is on the dispersion of the ash cloud and not on the absolute concentrations of particles as the emission source strength of the volcano is based on rough estimates only.

Figure 12 shows ash concentrations from simulations with MCCM with a horizontal resolution of 25 km at a height of approximately 3.5 km above the ground. Due to the uncer-
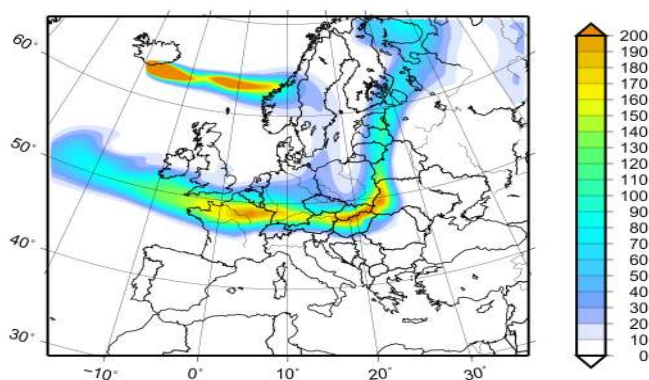


**Fig. 12.** Ash cloud distribution on 17 April 2010, 00:00 UTC at a height of approximately 3.5 km from MCCM simulations with 25 km horizontal resolution (first published by Wiegner et al., 2011). Colours give ash concentration in $\mu g \, m^{-3}$.

tainty of the amount of air borne ash emitted by the volcano, the concentrations given in Fig. 12 should not be considered as absolute values. A test simulation with a horizontal resolution of only 45 km has shown that the principal features of the transport of the ash plume are already reproduced for this resolution, although the patterns are less detailed and concentration maxima are less pronounced.

A time-height cross-section from the MCCM results for 16 to 21 April 2010 is shown in Fig. 13. The first two days can be compared to the ceilometer observations displayed in the lowest frame of Fig. 8. Except for a small bias towards a too early arrival, the time of the arrival of the bulk mass of the ash cloud in Southern Germany is in quite good agreement with the ceilometers measurements for both horizontal resolutions. However, the simulated ash cloud is much thicker than observed. This seems to be a feature that is also found for simulations of the ash cloud with other Eulerian models (e.g. Elbern, 2010). For the simulations shown here, this may mostly be attributed to the comparatively coarse vertical resolution that has been chosen in order to keep the numerical effort within reasonable limits. A test run where the number of model layers was increased by 10 to a total number of 43 resulted only a minor improvement of the simulated vertical structure of the ash cloud. In order to resolve structures with a vertical extension of only some hundred meters, a much better vertical resolution and a much higher numerical effort would be required. Another reason for the too large vertical extent of the simulated ash cloud might be the simple representation of the eruption plume.

The overall slanted shape of the ash cloud layer on 16 and 17 April is well depicted although the shallowness of the cloud is not reproduced. The temporal course of the ash clouds' bulk mass in Fig. 13 on the other hand agrees quite well with the ceilometer measurements, so that it may be assumed that the overall horizontal advection of the cloud in the model is not spoiled by too strong vertical diffusion. Horizontal advection is addressed further in the next Section.
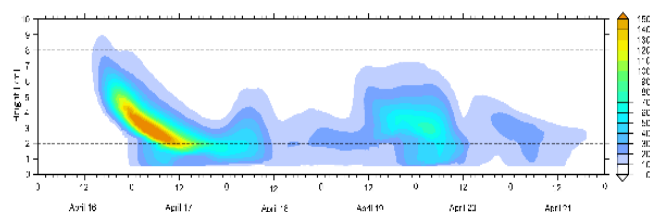
**Fig. 13.** Time-height section of the ash concentration in µg m$^{-3}$ from MCCM simulations for the area of Munich for 16 April to 21 April 2010.

Figure 13 also shows a second increase in ash concentrations on the afternoon of 19 April. This second event fits quite well to the ultralight aircraft observation described in Sect. 5.2 above. The ultralight aircraft, however, observed the arrival of the second plume around 15 UTC whereas an arrival time around 17 UTC was simulated by MCCM. But given the large distance the ash cloud has been advected from Iceland the previous five days, the arrival time simulations give errors of a few percent only. A test simulation where only the emissions of the first eruption day were considered indicates that over 50% of the ash observed on 19 and 20 April west of Munich was emitted on 14 April and was advected back to this region.

Figure 14 compares the arrival times at 3 km a.s.l. of the first ash cloud over Europe on 16 and 17 April 2010 from DWD ceilonet observations and numerical modelling with MCCM. The height of 3 km was chosen for this comparison in order to reduce ceilometer measurement errors resulting from the presence of clouds. Only the arrival time of this first and intense flush of ash was clearly deducible from the DWD ceilonet. Later flushes were still visible but due to clouds and missing sharp ash fronts, no exact arrival time could be inferred from the ceilonet instruments. The comparison in Fig. 14 shows general agreement between observations and the simulated arrival of the bulk mass of the ash. Smaller deviations are partly due to the presence of clouds which obstructed the ceilometers' view of the leading edge of the ash clouds at some locations. The decelerated ash cloud movement over Southwestern Germany is simulated properly, but the simulated cloud arrives a few hours earlier than that observed over Southeastern Germany. Further, the ash transport across the northern Alps on 17 April is modelled somewhat too fast, probably due to a lack of decelerating orographic impact at the lower levels due to the smoothed and flattened representation of the topography at 25 km horizontal resolution in the model (compare Figs. 8 and 13).

## 7 Conclusions

The eruption of volcanoes itself is still unpredictable, but once the ash cloud has been emitted, ground-based observations and numerical predictions of the dispersion of the cloud are possible. There is a fundamental need for reliable predic-
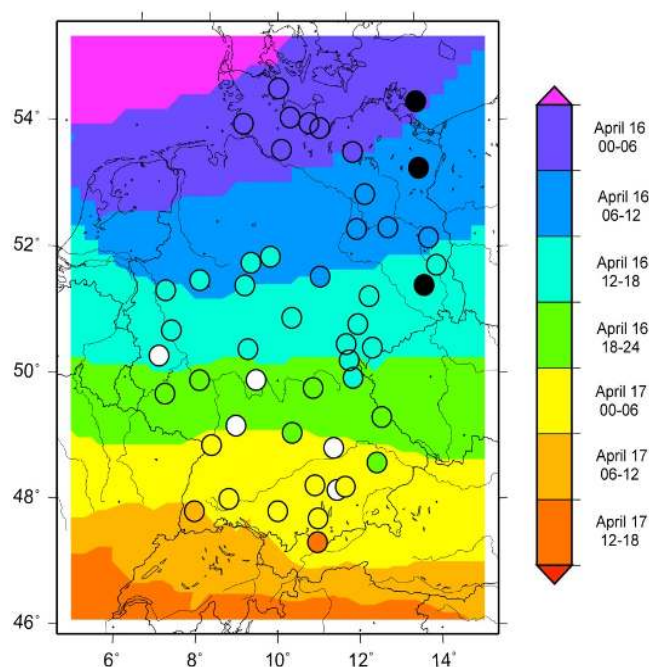


**Fig. 14.** Comparison of the arrival time of the first ash cloud over Europe on 16 and 17 April 2010 from ceilometer observations from the DWD ceilonet (circles) and from MCCM simulation (shading). The arrival times refer to 3 km height. The colours indicate the arrival times (6 h intervals, scale to the right). Black circles indicate sites without measurements, white circles that no ash cloud could be detected at this site.

tions for air traffic security reasons as well as for air quality aspects.

This study has shown that the first ash cloud arriving over Germany on 16/17 April 2010 was a quite shallow polluted layer which was only several hundreds of metres deep and which was oriented slantwise in the troposphere. In this layer, the aerosol concentration was so large that this layer could easily be followed by simple ground-based optical remote sensing instruments such as ceilometers. A quantification of concentration thresholds needed for a detection of ash clouds by ceilometers could not be derived from the available data due to the absence of continuous in-situ concentration data. The observation of later flushes of the ash cloud with lesser concentrations was partly disturbed by cloudy weather as well. Generally, ceilometers only give meaningful results during clear sky conditions in the lower and middle troposphere.

It is important to note with respect to volcanic ash detection that ceilometer information needs support from additional measurements for the identification of the volcanic origin of detected aerosol clouds. Ceilometers only give range-corrected backscatter information. Depolarisation measurements seem to be a good means for this, but back trajectories might also be helpful.

The apparent sinking of the ash cloud with time in the time-height sections derived from ceilometer observations

needs additional interpretation. The slantwise oriented ash cloud was subject to large-scale sinking motion during its advection over Germany. Therefore, the rapid apparent sinking of the ash cloud signal in single ceilometer time-height sections is due to two reasons: the large-scale sinking and the advection of an inclined layer which is at lower altitudes at its rear end.

Eulerian numerical models are a good means to predict the dispersion of the ash clouds. The comparison presented here has shown the principal ability of such a model to perform this task. The progression of the leading edge of the first flush of the ash was simulated quite well. Even after about 120 h simulation time, the difference to the measurement of the arrival time of a new flush of ash is only about 2 h, which is an error of less than two percent. Simultaneously, this study has shown that an evaluation of dispersion models is possible with a ground-based optical remote sensing network of ceilometers. The case presented here is presumably the first example of a comparison between a numerical model result and data from a ceilometer network.

Mountainous terrain seems to have a considerable influence on ash cloud dispersion. Due to the enhanced and modified vertical motions over such terrain, vertical dilution of the ash cloud is much stronger over mountainous terrain. Therefore, lower tropospheric aerosol clouds might easily lose their identity when they have to pass larger mountain chains. It is proposed that this is one of the reasons why there appeared to be a difference between the simulated and observed progression of the leading edge of the ash layer close to the Alps. This issue needs further consideration in future.

The above results indicate that for air traffic security, the combination of a modern dispersion model together with a well-designed ceilometer network which is supported by special profiling measurements (depolarisation, spectral aerosol properties) may be a good means to predict the dispersion of thicker volcanic ash clouds. Reliable estimates of ash particle concentrations within the ash clouds from such dispersion models require good estimates of the emission strength of the volcano and the particle size spectrum. Whether this is sufficient to avoid aircraft hazards has to be investigated in more detail later when threshold values for hazardous ash concentrations are available from engineering sciences.

## References

Amt der Tiroler Landesregierung: Monthly report of air pollution in Tirol, April 2010, available at: http://www.tirol.gv.at/uploads/media/Monatsbericht_April_2010.pdf.

Ansmann, A., Bösenberg, J., Chaikovsky, A., Comerón, A., Eckhardt, S., Eixmann, R., Freudenthaler, V., Ginoux, P., Komguem, L., Linné, H., López Márquez, M. Á., Matthias, V., Mattis, I., Mitev, V., Müller, D., Music, S., Nickovic, S., Pelon, J., Sauvage, L., Sobolewsky, P., Srivastava, M. K., Stohl, A., Torres, O., Vaughan, G., Wandinger, U., and Wiegner, M.: Long-range transport of Saharan dust to northern Europe: The 11–16 October 2001 outbreak observed with EARLINET, J. Geophys. Res., 108(D24), 4783, doi:10.1029/2003JD003757, 2003.

Birmili, W., Weinhold, K., Nordmann, S., Wiedensohler, A., Spindler, G., Müller, K., Herrmann, H., Gnauk, T., Pitz, M., Cyrys, J., Flentje, H., Nickel, C., Kuhlbusch, T. A. J., Löschau, G., Haase, D., Meinhardt, F., Schwerin, A., Ries, L., and Wirtz, K.: Atmospheric aerosol measurements in the German Ultrafine Aerosol Network (GUAN): Part 1 – soot and particle number size distributions, Gefahrst. Reinh. Luft, 69, 137–145, 2009.

Bösenberg, J., Matthias, V., Amodeo, A., Amoiridis, V., Ansmann, A., Baldasano, J. M., Balin, I., Balis, D., Böckmann, C., Boselli, A., Carlsson, G., Chaikovsky, A., Chourdakis, G., Comerón, A., De Tomasi, F., Eixmann, R.,Freudenthaler, V., Giehl, H., Grigorov, I., Hågård, A., Iarlori, M., Kirsche, A., Kolarov, G., Komguem, L., Kreipl, S., Kumpf, W., Larchevêque, G., Linné, H., Matthey, R., Mattis, I., Mekler, A., Mironova, I., Mitev, V., Mona, L., Müller, D., Music, S., Nickovic, S., Pandolfi, M., Papayannis, A., Pappalardo, G., Pelon, J., Pérez, C., Perrone, R. M., Persson, R., Resendes, D. P., Rizi, V., Rocadenbosch, F., Rodrigues, J. A., Sauvage, L., Schneidenbach, L., Schumacher, R., Shcherbakov, V., Simeonov, V., Sobolewski, P., Spinelli, N., Stachlewska, I., Stoyanov, D., Trickl, T., Tsaknakis, G., Vaughan, G., Wandinger, U., Wang, X., Wiegner, M., Zavrtanik, M., and Zerefos, C.: EARLINET: A European aerosol research lidar network to establish an aerosol climatology. MPI-Report 348, Max-Planck-Institute for Meteorology, Hamburg, Germany, 191 pp., ISSN 0937-1060, available at: http://www.mpimet.mpg.de/fileadmin/publikationen/Reports/max_scirep_348.pdf, 2003.

Casadevall, T. J.: Volcanic hazards and aviation safety – Lessons of the past decade, FAA Aviation Safety J., 2, 9–17, 1992.

Damoah, R., Spichtinger, N., Forster, C., James, P., Mattis, I., Wandinger, U., Beirle, S., Wagner, T., and Stohl, A.: Around the world in 17 days – hemispheric-scale transport of forest fire smoke from Russia in May 2003, Atmos. Chem. Phys., 4, 1311–1321, doi:10.5194/acp-4-1311-2004, 2004.

Durand, M. and Grattan, J.: Effects of volcanic air pollution on health, The Lancet, 357, 164, 2001.

Elbern, H.: R&D modelling/forecasting of the Eyjafjöll ash plume at University of Cologne. Talk at the ESA/EUMETSAT Workshop on Volcanic Ash Plume Monitoring on 26/27 May 2010 at Frascati (Rome), http://earth.eo.esa.int/workshops/Volcano/files/8_Elbern_Eyjafjalla_ESA.pdf, 2010.

Emeis, S.: Measurement Methods in Atmospheric Sciences. In situ and remote. Series: Quantifying the Environment, Vol. 1, Borntraeger Stuttgart, ISBN 978-3-443-01066-9, 2010.

Flentje, H., Heese, B., Reichardt, J., and Thomas, W.: Aerosol profiling using the ceilometer network of the German Meteorological Service, Atmos. Meas. Tech. Discuss., 3, 3643–3673,

doi:10.5194/amtd-3-3643-2010, 2010a.

Flentje, H., Claude, H., Elste, T., Gilge, S., Köhler, U., Plass-Dülmer, C., Steinbrecht, W., Thomas, W., Werner, A., and Fricke, W.: The Eyjafjallajökull eruption in April 2010 – detection of volcanic plume using in-situ measurements, ozone sondes and lidar-ceilometer profiles, Atmos. Chem. Phys., 10, 10085–10092, doi:10.5194/acp-10-10085-2010, 2010b.

Freudenthaler, V., Esselborn, M., Wiegner, M., Heese, B., Tesche, M., Ansmann, A., Müller, D., Althausen, D., Wirth, M., Fix, A., Ehret, G., Knippertz, P., Toledano, C., Gasteiger, J., Garhammer, M., and Seefeldner, M.: Depolarization ratio profiling at several wavelengths in pure Saharan dust during SAMUM 2006. Tellus 61B, 165–179, 2009.

Furger, F., Dommen, J., Graber, W. K., Poggio, L., Prévôt, A., Emeis, S., Trickl, T., Grell, G., Neininger, B., and Wotawa, G.: The VOTALP Mesolcina Valley Campaign 1996 – Concept, Background and some Highlights, Atmos. Environ., 34, 1395–1412, 2000.

Grattan, J. and Brayshay, M.: An Amazing and Portentous Summer: Environmental and Social Responses in Britain to the 1783 Eruption of an Iceland Volcano, The Geographical Journal, 161, 125–134, 1995.

Grell, G. A., Dudhia, J., and Stauffer, D. R.: A description of the Fifth-generation Penn State/NCAR Mesoscale Model (MM5), NCAR Tech Note TN-398#STR, 122 pp., 1994.

Grell, G. A., Emeis, S., Stockwell, W. R., Schoenemeyer, T., Forkel, R., Michalakes, J., Knoche, R., and Seidl, W.: Application of a multiscale, coupled MM5/Chemistry Model to the complex terrain of the VOTALP Valley Campaign, Atmos. Environ., 34, 1435–1453, 2000.

Grutter, M., Basaldud, R., Rivera, C., Harig, R., Junkerman, W., Caetano, E., and Delgado-Granados, H.: $SO_2$ emissions from Popocatpetl volcano: emission rates and plume imaging using optical remote sensing techniques, Atmos. Chem. Phys., 8, 6655–6663, doi:10.5194/acp-8-6655-2008, 2008.

Haas, E., Forkel, R., and Suppan, P.: Application and intercomparison of the RADM2 and RACM chemistry mechanism including a new isoprene degradation scheme within the regional meteorology-chemistry-model MCCM, Int. J. Environ. Pollut., 40, 1/2/3, 236–148, 2010.

ICAO: International Civil Aviation Organisation International Handbook on the International Airways Volcano Watch (IAVW) – Operational procedures and contact list, ICAO Doc 9766-AN/968, First Edition, 2000.

Junkermann, W.: An Ultralight Aircraft as Platform for Research in the Lower Troposphere: System Performance and First Results from Radiation Transfer Studies in Stratiform Aerosol Layers and Broken Cloud Conditions, J. Atmos. Oceanic Technol., 18, 934–946, 2001.

Petersen, G. N.: A short meteorological overview of the Eyjafjallajökull eruption 14 April–23 May 2010, Weather, 65(8), 203–207, 2010.

Pollack, J. B., Toon, O. B., Ackerman, T. P., McKay, C. P., and Turco, R. P.: Environmental Effects of an Impact-Generated Dust Cloud: Implications for the Cretaceous-Tertiary Extinctions, Science, 219(4582), 287–289, 1983.

Schäfer, K., Thomas, W., Peters, A., Ries, L., Obleitner, F., Schnelle-Kreis, J., Birmili, W., Diemer, J., Fricke, W., Junkermann, W., Pitz, M., Emeis, S., Forkel, R., Suppan, P., Flentje, H., Wichmann, H. E., Gilge, S., Meinhardt, F., Zimmermann, R., Weinhold, K., Soentgen, J., Münkel, C., Freuer, C., and Cyrys, J.: Influences of the 2010 Eyjafjallaj—"okull volcanic plume on air quality in the northern Alpine region, Atmos. Chem. Phys. Discuss., 11, 9083–9132, doi:10.5194/acpd-11-9083-2011, 2011.

Schell, B., Ackermann, I. J., Hass, H., Binkowski, F. S., and Ebel, A.: Modeling the formation of secondary organic aerosol within a comprehensive air quality model system, J. Geophys. Res., 106, 28275–28293, 2001.

Schreiter M.: Auswertung von Ceilometerdaten hinsichtlich Grenzschicht- und Wolkenhöhe im Raum Innsbruck und Wien, Diploma thesis submitted at Institute of Meteorology and Geophysics, Innsbruck University, 2010.

Schumann, U., Weinzierl, B., Reitebuch, O., Schlager, H., Minikin, A., Forster, C., Baumann, R., Sailer, T., Graf, K., Mannstein, H., Voigt, C., Rahm, S., Simmet, R., Scheibe, M., Lichtenstern, M., Stock, P., Rüba, H., Schäuble, D., Tafferner, A., Rautenhaus, M., Gerz, T., Ziereis, H., Krautstrunk, M., Mallaun, C., Gayet, J.-F., Lieke, K., Kandler, K., Ebert, M., Weinbruch, S., Stohl, A., Gasteiger, J., Olafsson, H., and Sturm, K.: Airborne observations of the Eyjafjalla volcano ash cloud over Europe during air space closure in April and May 2010, Atmos. Chem. Phys. Discuss., 10, 22131–22218, doi:10.5194/acpd-10-22131-2010, 2010.

Shao, Y.: Physics and Modelling of Wind Erosion, 2nd Edn. (revised and expanded), Atmospheric and Oceanographic Sciences Library, Springer, 452 pp., 2008.

Simpson, J. J., Hufford, G. L., Servranckx, R., Berg, J., and Pieri, D.: Airborne Asian Dust: Case Study of Long-Range Transport and Implications for the Detection of Volcanic Ash, Weather Forecast., 18, 121–141, 2003.

Stockwell, W. R., Middleton, P., Chang, J. S., and Tang, X.: The second generation regional acid deposition model chemical mechanism for regional air quality modeling, J. Geophys. Res., 95, 16343–16367, 1990.

Tupper, A., Davey, J., Stewart, P., Stunder, B., Servranckx, R., and Prata, F.: Aircraft encounters with volcanic clouds over Micronesia, Oceania, 2002–03, Aust. Met. Mag., 55, 289–299, 2006.

Wiegner, M., Gasteiger, J., Groß, S., Schnell, F., Freudenthaler, V., and Forkel, R.: Characterization of the Eyjafjallajökull ash-plume: Potential of lidar remote sensing, Phys. Chem. Earth, doi:10.1016/j.pce.2011.01.006, in press, 2011.

Witham, C. S., Hort, M. C., Potts, R., Servranckx, R., Husson, P., and Bonnardot, F.: Comparison of VAAC atmospheric dispersion models using the 1 November 2004 Grimsvötn eruption, Meteorol. Appl., 14, 27–38, 2007.

Woods, A. W., Holasek, R. E., and Self, S.: Wind-driven dispersal of volcanic ash plumes and its control on the thermal structure of the plume-top, Bull. Volcanol., 57, 283–292, 1995.